

# Superconducting energy gaps, low temperature specific heat, and quasiparticle spectra of $\text{MgB}_2$

Hyoung Joon Choi,<sup>\*</sup> David Roundy,<sup>\*†</sup> Hong Sun,<sup>\*</sup> Marvin L. Cohen,<sup>\*†</sup> & Steven G. Louie<sup>\*†</sup>

<sup>\*</sup>*Department of Physics, University of California at Berkeley, Berkeley, CA 94720, USA.*

<sup>†</sup>*Materials Sciences Division, Lawrence Berkeley National Laboratory, Berkeley, CA 94720, USA.*

Magnesium diboride is remarkable not only for its unusually high transition temperature of 39K for a *sp*-bonded metal [1] and its reduced isotope-effect exponent [2,3], but also for its unusual superconducting gap behavior [4–16]. Some earlier experiments seem consistent with conventional single-gap superconductivity [4–8], but recent measurements indicate the existence of more than one gap [9–16]. For example, specific heat measurements show an anomalous large bump at low temperature, inconsistent with single-gap BCS theory. Moreover, there is a significant variation in the measured values for the gaps. Here, we report first-principles calculations of the  $k$ - and  $T$ -dependent superconducting gap  $\Delta(\vec{k}, T)$  in  $\text{MgB}_2$  and its manifestation in various measured quantities. Because its Fermi surface has disconnected sheets with very different electron-phonon coupling strengths, our calculations show that near  $T = 0$ , the values of  $\Delta(\vec{k})$  cluster into two groups: large values ( $\sim 6.5$  to  $7.5$  meV) on the strongly coupled sheets and small values ( $\sim 1$  to  $3$  meV) on the weakly coupled sheets. The calculated gap, quasiparticle density of states, and specific heat and their temperature dependences are in agreement with the recent measurements which support that  $\text{MgB}_2$  is a multiple gap superconductor. In fact, theory predicts four prominent values for the gap at low  $T$ .

Most theoretical work on  $\text{MgB}_2$  has been focused on the electronic structure, the phonon structure, and the electron-phonon interaction [17–23]. It is shown that the electron-phonon

interaction in  $\text{MgB}_2$  varies strongly on the Fermi surface [21–23]. Also, recent two-band model [21] and first-principles [23] studies of the transition temperature support a multi-gap scenario [24]. However, no detailed quantitative calculations have been presented for the temperature and  $k$ -space dependence of the superconducting gap. The calculational framework [23] used here is based on the strong coupling formalism of superconductivity established by Eliashberg [25,26]. The Eliashberg formalism is a more general case of the original formulation of the BCS theory for phonon-mediated pairing, taking into account strong electron-phonon coupling. When applying the strong coupling theory to  $\text{MgB}_2$ , we include the momentum dependency of the anisotropic Eliashberg equation and also take into account the anharmonic effect on phonon frequencies. Material-dependent parameters in the equation are obtained by *ab initio* pseudopotential density functional calculations. This approach has already been shown to describe the superconducting transition of  $\text{MgB}_2$  very accurately; the obtained specific heat mass enhancement factor  $\lambda = 0.61$ , the transition temperature  $T_c = 39\text{K}$ , and isotope-effect exponent  $\alpha_B = 0.31$  are all in excellent agreement with experiments [23]. Here, we compute the gap function  $\Delta(\vec{k}, \omega)$  and the renormalization factor  $Z(\vec{k}, \omega)$  from the fully anisotropic Eliashberg equation at various temperatures. This allows us to address all the superconducting properties except those related to the presence of an applied magnetic field.

Figure 1 shows the calculated superconducting gap  $\Delta(\vec{k})$  on the Fermi surface at 4 K. The Fermi surface of  $\text{MgB}_2$  consists of four sheets: two-dimensional (2D) light hole and heavy hole sheets forming coaxial cylinders along  $\Gamma$  to  $A$ , a three-dimensional (3D) hole sheet connecting regions near  $K$  and  $M$ , and a 3D electron sheet connecting regions near  $H$  and  $L$ . The 2D light and heavy hole sheets are derived from  $\sigma$ -antibonding states of boron  $p_{x,y}$  orbitals, while the 3D hole and electron sheets are derived from  $\pi$ -bonding and antibonding states of boron  $p_z$  orbitals, respectively. The calculated density of states at the Fermi energy is 0.115 states/eV·atom·spin; 44 % of which comes from the 2D  $\sigma$  cylindrical sheets and the rest comes from the 3D  $\pi$  sheets. The superconducting gap is nonzero everywhere on the Fermi surface. Thus, the symmetry of the superconducting gap is s-

wave, but the size of the gap changes on the Fermi surface. The gap values cluster into two groups. The largest gap is on the 2D light hole  $\sigma$  cylindrical sheet (shown red in Fig. 1), where the average gap is 7.2 meV with variations of less than 0.1 meV. On the 2D heavy hole  $\sigma$  cylindrical sheet (shown orange in Fig. 1), the superconducting gap ranges from 6.4 meV to 6.8 meV, having an average of 6.6 meV, with maximum value near  $\Gamma$  and minimum value near A. The average of the gap values on the two 2D  $\sigma$  cylindrical sheets is 6.8 meV. The superconducting gap is significantly smaller and more spread out on the 3D  $\pi$  sheets (shown green and blue in Fig. 1), ranging from 1.2 meV to 3.7 meV. Out of the two 3D  $\pi$  sheets, the hole sheet shows a slightly larger gap with a peak at 2.1 meV and the electron sheet shows a somewhat smaller gap with a peak at 1.5 meV. The average of the gap values on the two 3D  $\pi$  sheets is 1.8 meV. This very large variation in the gap value originates from the differences in electron-phonon coupling strengths on the different sheets of the Fermi surface. Our *ab initio* calculations [23] demonstrate that the electron-phonon coupling strength is 4 to 5 times stronger on the cylindrical  $\sigma$  sheets (exceeding 2.5 for some states) than on the  $\pi$  sheets. Our result is consistent with the recent experiments reporting two gaps [9–16] because the superconducting gap in MgB<sub>2</sub> can be grossly viewed as consisting of a large gap of  $\sim 6.8$  meV on the strongly coupled 2D  $\sigma$ -cylindrical sheets and a small gap of  $\sim 1.8$  meV on the weakly coupled 3D  $\pi$  sheets. However, this simplification is limited. As seen in Fig. 1, the large and small gaps both have substantial variation in value: 6.4 to 7.2 meV on the 2D  $\sigma$  sheets and 1.2 to 3.7 meV on the 3D  $\pi$  sheets. The experimental interpreted gaps have a range of 1.5 to 3.5 meV for the small gap and a range of 5.5 to 8 meV for the large gap [9–16,27].

Figure 2 shows the temperature dependence of the superconducting energy gap on the Fermi surface from 4K to 38K which may be probed in tunneling, optical, and specific heat measurements. The vertical blue curves in Fig. 2 present the distribution of the superconducting gap values at various temperatures, and the red lines are curves of the form  $\Delta(T) = \Delta(0)\sqrt{1 - (T/T_c)^p}$  fitted separately to the averaged values of the calculated gap on the 2D  $\sigma$  sheets and those on the 3D  $\pi$  sheets. Our calculated results give  $\Delta(0) = 6.8$  meV

( $2\Delta(0)/k_B T_c = 4.0$ ) for the averaged gap at  $T = 0$  on the 2D  $\sigma$  sheets, and  $\Delta(0) = 1.8$  meV ( $2\Delta(0)/k_B T_c = 1.06$ ) for that on the 3D  $\pi$  sheets. The theory shows that the superconducting gap opens at  $T_c$  throughout the Fermi surface, and that the gap widens much faster on the 2D  $\sigma$  sheets than on the 3D  $\pi$  sheets at  $T \lesssim T_c$ .

From the calculated gap function  $\Delta(\vec{k}, \omega)$ , the quasiparticle density of states is given by

$$N(\omega)/N(0) = \text{Re} \left\langle \frac{\omega + i\Gamma}{\sqrt{(\omega + i\Gamma)^2 - \Delta(\vec{k}, \omega)^2}} \right\rangle, \quad (1)$$

where  $\langle \dots \rangle$  indicates an average over a surface of constant  $\omega$ . Figure 3 depicts the theoretical quasiparticle density of states calculated with an assumed finite lifetime  $\Gamma$  of 0.1 meV. The quasiparticle density of states at 4K shows three discernable peaks. One peak is at 2.2 meV, which is slightly greater than the dominant size of the gap (2.1 meV) on the 3D  $\pi$  hole sheet. The other two peaks are at 6.8 and 7.2 meV, which are the maximal sizes of the superconducting gap on the 2D heavy and light hole  $\pi$  sheets, respectively. The quasiparticle density of states can be deduced from tunneling experiments and various spectroscopic measurements [9–11,15,16], but a direct quantitative comparison requires knowledge of various physical parameters involved in a specific experiment.

A fundamental measurement which can provide a probe of the superconducting quasiparticle spectrum is the temperature-dependent specific heat. Figure 4 shows the calculated  $T$ -dependent specific heat of MgB<sub>2</sub> through the superconducting transition. For the normal-state specific heat  $C_N = \gamma T$ , we obtain  $\gamma = 2.62$  mJ/mol·K<sup>2</sup> [23], which agrees well with experimental values 2.6 mJ/mol·K<sup>2</sup> [13] and 2.7 mJ/mol·K<sup>2</sup> [12,14]. For the superconducting-state specific heat  $C_S$ , we first calculate the free energy difference ( $F_S - F_N$ ) of the superconducting and normal states [28] and then obtain the specific heat difference by

$$C_S - C_N = -T \frac{d^2}{dT^2} (F_S - F_N). \quad (2)$$

The measured low  $T$  specific heat [12–14] shows substantial magnitude and a large bump at about 10K. This anomalous behavior is inconsistent with a 1-gap BCS model. However, our

results are in excellent agreement with experiment. The origin of the bump in our calculated curve is the existence of low energy excitations above the small gap on the weakly coupled 3D  $\pi$  sheets of the Fermi surface. The overall shape and magnitude of the calculated specific heat curve agrees very well with experiments, especially below 30K, and shows a jump of  $\Delta C/\gamma T_c = 1.0$  at  $T_c$  which is within the range of the measured values.

## REFERENCES

- [1] Nagamatsu, J., Nakagawa, N., Muranaka, T., Zenitani, Y. & Akimitsu, J. Superconductivity at 39K in magnesium diboride. *Nature* **410**, 63-64 (2001).
- [2] Bud'ko, S.L. *et al.* Boron isotope effect in superconducting MgB<sub>2</sub>. *Phys. Rev. Lett.* **86**, 1877-1880 (2001).
- [3] Hinks, D.G., Claus, H. & Jorgensen, J.D. The complex nature of superconductivity in MgB<sub>2</sub> as revealed by the reduced total isotope effect. *Nature* **411**, 457-460 (2001).
- [4] Karapetrov, G., Iavarone, M., Kwok, W.K., Crabtree, G.W. & Hinks, D.G. Scanning tunneling spectroscopy in MgB<sub>2</sub>. *Phys. Rev. Lett.* **86**, 4374-4377 (2001).
- [5] Sharoni, A., Felner, I. & Millo, O. Tunneling spectroscopy and magnetization measurements of the superconducting properties of MgB<sub>2</sub>. *Phys. Rev. B* **63**, 220508 (2001).
- [6] Rubio-Bollinger, G., Suderow, H. & Vieira, S. Tunneling spectroscopy in small grains of superconducting MgB<sub>2</sub>. *Phys. Rev. Lett.* **86**, 5582-5584 (2001).
- [7] Schmidt, H., Zasadzinski, J.F., Gray, K.E. & Hinks, D.G. Energy gap from tunneling and metallic contacts onto MgB<sub>2</sub>: possible evidence for a weakened surface layer. *Phys. Rev. B* **63**, 220504 (2001).
- [8] Takahashi, T., Sato, T., Souma, S., Muranaka, T. & Akimitsu, J. High-resolution photoemission study of MgB<sub>2</sub>. *Phys. Rev. Lett.* **86**, 4915-4917 (2001).
- [9] Szabo, P. *et al.* Evidence for two superconducting energy gaps in MgB<sub>2</sub> by point-contact spectroscopy. *Phys. Rev. Lett.* **87**, 137005 (2001).
- [10] Giubileo, F. *et al.* Two-gap state density in MgB<sub>2</sub>: a true bulk property or a proximity effect? *Phys. Rev. Lett.* **87**, 177008 (2001).
- [11] Laube, F. *et al.*, Superconducting energy gap distribution of MgB<sub>2</sub> investigated by point-contact spectroscopy. Preprint cond-mat/0106407 at <<http://xxx.lanl.gov>> (2001).

- [12] Wang, Y., Plackowski, T. & Junod, A. Specific heat in the superconducting and normal state (2-300K, 0-16 T), and magnetic susceptibility of the 38 K superconductor  $\text{MgB}_2$ . *Physica C* **355**, 179-193 (2001).
- [13] Bouquet, F., Fisher, R.A., Phillips, N.E., Hinks, D.G. & Jorgensen, J.D. Specific heat of  $\text{Mg}^{11}\text{B}_2$ : evidence for a second energy gap. *Phys. Rev. Lett.* **87**, 47001 (2001).
- [14] Yang, H.D., Lin, J.-Y., Li, H.H., Hsu, F.H., Liu, C.J., Li, S.-C., Yu, R.-C. & Jin, C.-Q. Order parameter of  $\text{MgB}_2$ : a fully gapped superconductor. *Phys. Rev. Lett.* **87**, 167003 (2001).
- [15] Chen, X.K., Konstantinovi, M.J., Irwin, J.C., Lawrie, D.D. & Franck, J.P. Evidence for two superconducting gaps in  $\text{MgB}_2$ . *Phys. Rev. Lett.* **87**, 157002 (2001).
- [16] Tsuda, S. *et al.* Evidence for a multiple superconducting gap in  $\text{MgB}_2$  from high-resolution photoemission spectroscopy. *Phys. Rev. Lett.* **87**, 177006 (2001).
- [17] Kortus, J., Mazin, I.I., Belashchenko, K.D., Antropov, V.P. & Boyer, L.L. Superconductivity of metallic boron in  $\text{MgB}_2$ . *Phys. Rev. Lett.* **86**, 4656-4659 (2001).
- [18] An, J.M. & Pickett, W.E. Superconductivity of  $\text{MgB}_2$ : covalent bonds driven metallic. *Phys. Rev. Lett.* **86**, 4366-4369 (2001).
- [19] Bohnen, K.-P., Heid, R. & Renker, B. Phonon dispersion and electron-phonon coupling in  $\text{MgB}_2$  and  $\text{AlB}_2$ . *Phys. Rev. Lett.* **86**, 5771-5774 (2001).
- [20] Yildirim, T. *et al.* Giant anharmonicity and nonlinear electron-phonon coupling in  $\text{MgB}_2$ : a combined first-principles calculation and neutron scattering study. *Phys. Rev. Lett.* **87**, 37001 (2001).
- [21] Liu, A.Y., Mazin, I.I. & Kortus, J. Beyond Eliashberg superconductivity in  $\text{MgB}_2$ : anharmonicity, two-phonon scattering, and multiple gaps. *Phys. Rev. Lett.* **87**, 87005 (2001).

- [22] Kong, Y., Dolgov, O.V., Jepsen, O. & Andersen, O.K. Electron-phonon interaction in the normal and superconducting states of  $\text{MgB}_2$ . *Phys. Rev. B* **64** 20501 (2001).
- [23] Choi, H.J., Roundy, D., Sun, H., Cohen, M. L. & Louie, S.G. First-principles calculation of the superconducting transition in  $\text{MgB}_2$  within the anisotropic Eliashberg formalism. Preprint cond-mat/0111182 at <<http://xxx.lanl.gov>> (2001).
- [24] Suhl, H., Matthias, B.T. & Walker, L.R. Bardeen-Cooper-Schrieffer theory of superconductivity in the case of overlapping bands. *Phys. Rev. Lett.* **3**, 552-554 (1959).
- [25] Éliashberg, G.M. Interactions between electrons and lattice vibrations in a superconductor. *Zh. Eksp. Teor. Fiz.* **38**, 966-976 (1960); *Sov. Phys.-JETP(Engl. Transl.)* **11**, 696-702 (1960).
- [26] Allen, P.B. & Mitrović, B. Theory of superconducting  $T_c$ . in *Solid State Physics*, edited by Ehrenreich, H., Seitz, F., Turnbull, D. (Academic, New York 1982) **37**, 1-92, and references therein; Carbotte, J.P. Properties of boson-exchange superconductors. *Rev. Mod. Phys.* **62**, 1027-1157 (1990).
- [27] Buzea, C. & Yamashita, T. Review of superconducting properties of  $\text{MgB}_2$ . Preprint cond-mat/0108265 at <<http://xxx.lanl.gov>> (2001).
- [28] Bardeen, J. & Stephen, M. Free-energy difference between normal and superconducting states. *Phys. Rev.* **136**, A1485-A1487 (1964).

This work was supported by National Science Foundation Grant No. DMR00-87088, and by the Director, Office of Science, Office of Basic Energy Sciences of the U. S. Department of Energy under Contract DE-AC03-76F0098. Computational resources have been provided by the National Science Foundation at the National Center for Supercomputing Applications and by the National Energy Research Scientific Computing Center. Authors also acknowledge financial support from the Miller Institute (H.J.C.) and from the Berkeley Scholar Program funded by the Tang Family Foundation (H.S.).



Correspondence should be addressed to S.G.L. (e-mail: [sglouie@uclink.berkeley.edu](mailto:sglouie@uclink.berkeley.edu)).

# FIGURES

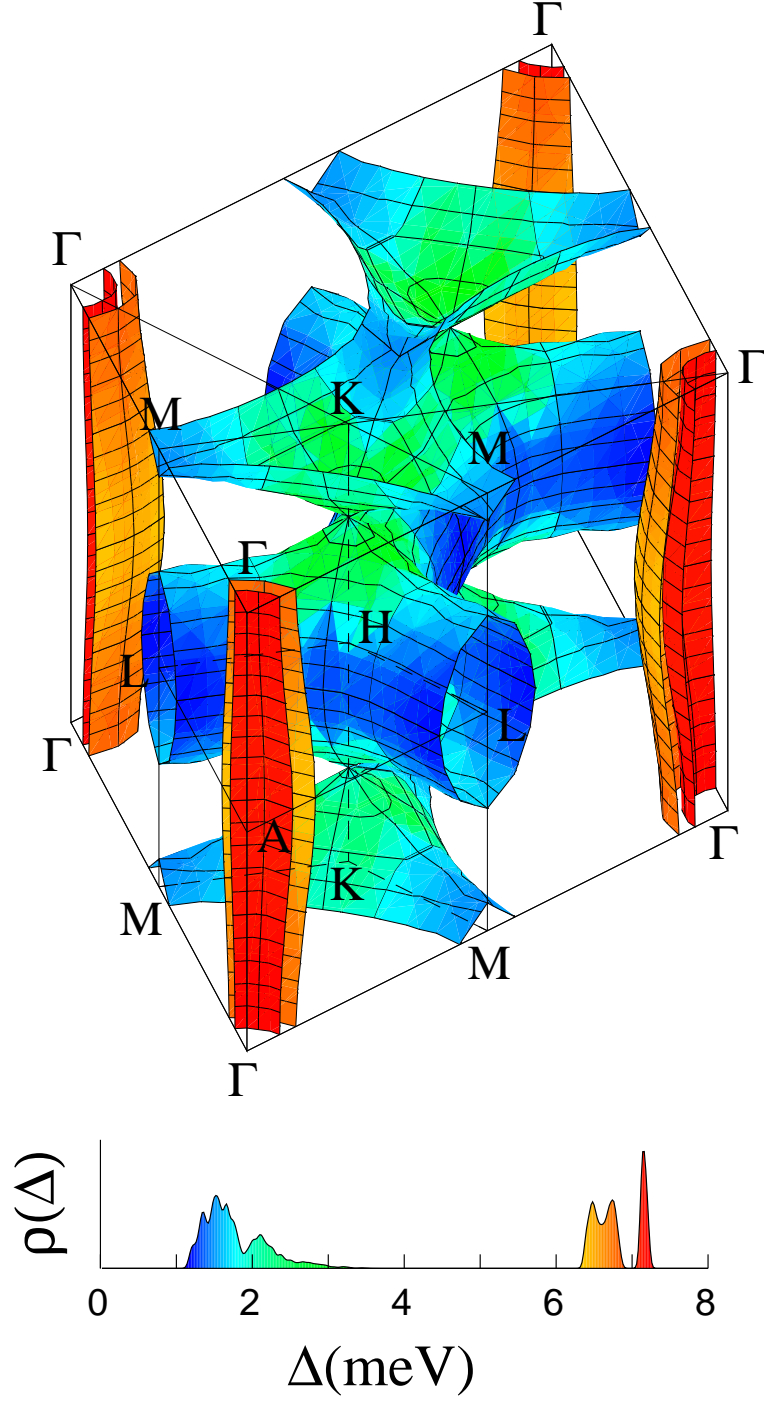


FIG. 1. (color) The superconducting energy gap on the Fermi surface at 4 K. Data is given in a color scale (top panel). The bottom panel depicts the distribution of gap values and the color scale used.

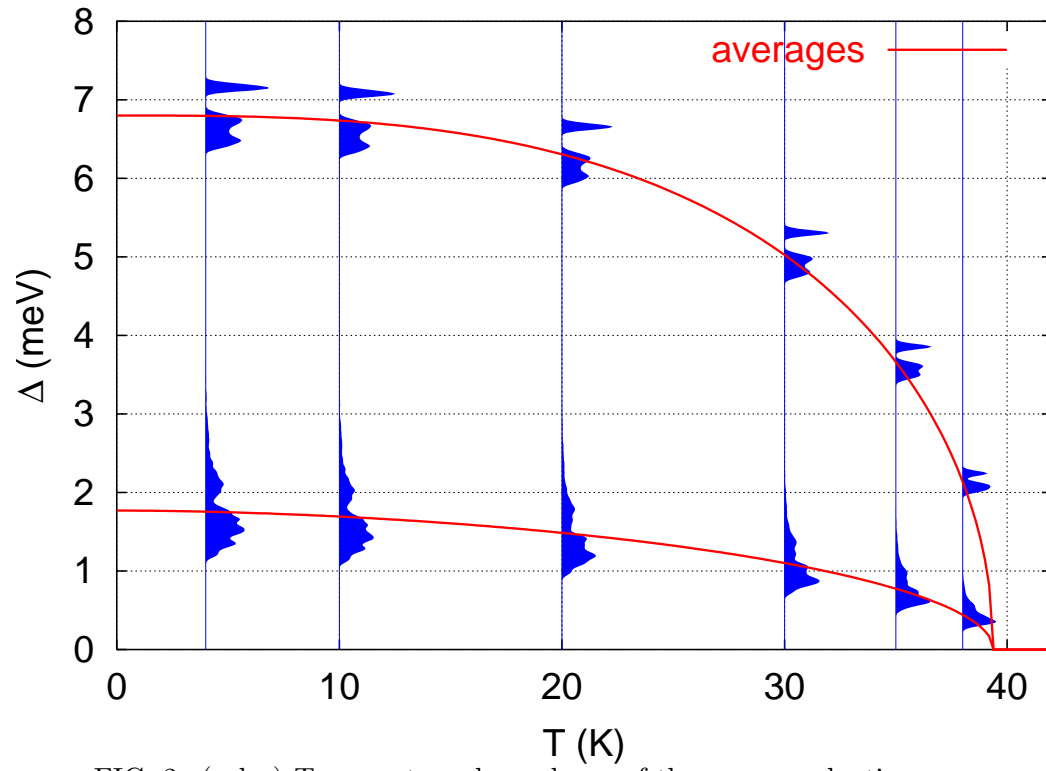


FIG. 2. (color) Temperature dependence of the superconducting gap.

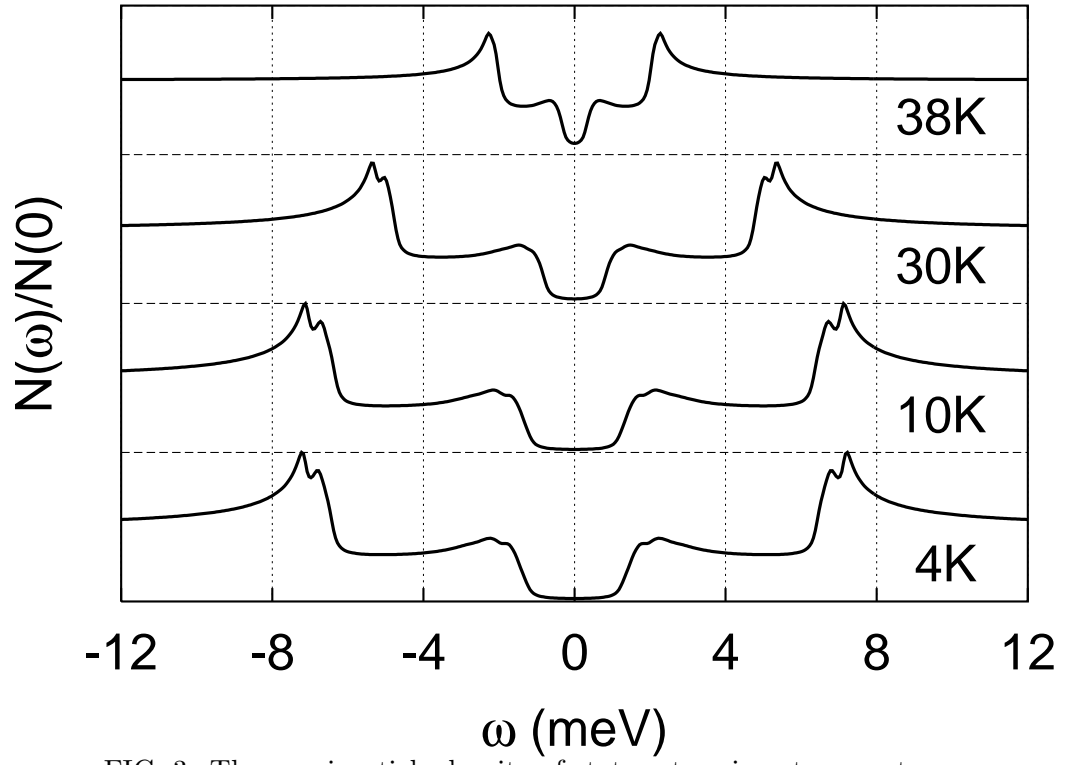


FIG. 3. The quasiparticle density of states at various temperatures.

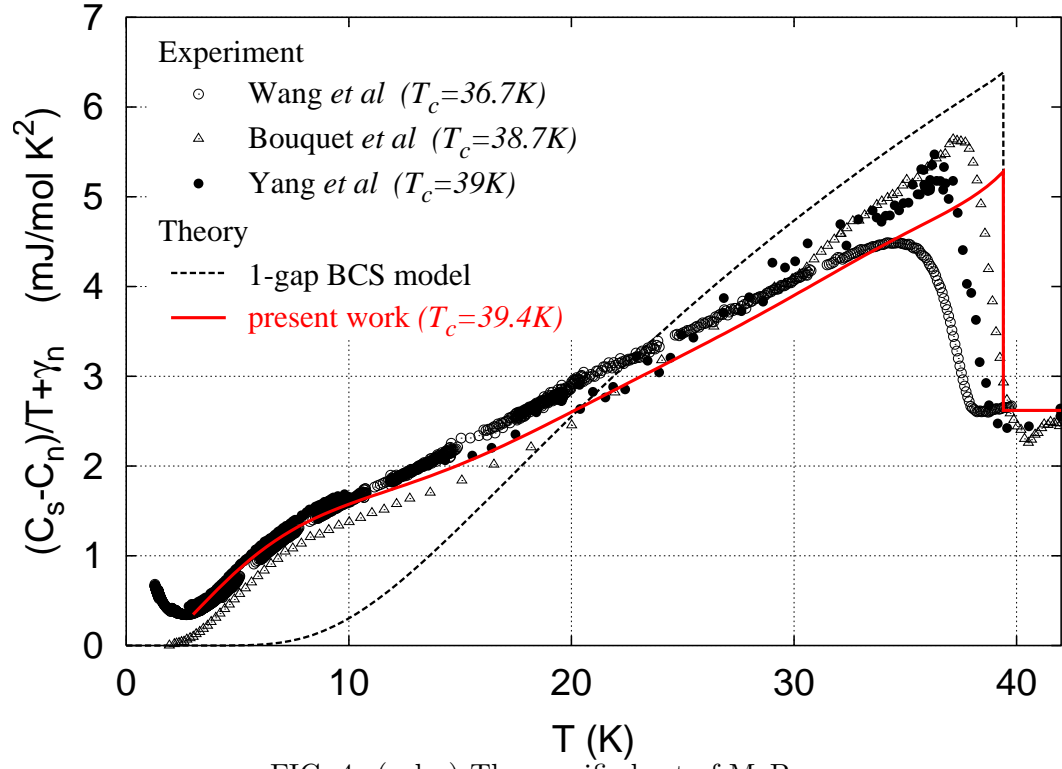


FIG. 4. (color) The specific heat of MgB<sub>2</sub>.